Cryobiology 69 (2014) 91–99

Contents lists available at ScienceDirect

Cryobiology

journal homepage: www.elsevier.com/locate/ycryo

Fluorescence as an alternative to light-scatter gating strategies to identify frozen–thawed cells with flow cytometry ☆

Anthony J.F. Reardon [a], Janet A.W. Elliott [a,b,*], Locksley E. McGann [a]

[a] Department of Laboratory Medicine and Pathology, University of Alberta, Edmonton, Alberta, Canada
[b] Department of Chemical and Materials Engineering, University of Alberta, Edmonton, Alberta, Canada

ARTICLE INFO

Article history:
Received 10 November 2013
Accepted 21 May 2014
Available online 29 May 2014

Keywords:
Flow cytometry
Light scattering
Fluorescence
Cryopreservation
Cryobiology
Cell gating
Membrane integrity
Mitochondria
Mitochondrial membrane potential
Human umbilical vein endothelial cells (HUVEC)

ABSTRACT

Flow cytometry is a key instrument in biological studies, used to identify and analyze cells in suspension. The identification of cells from debris is commonly based on light scatter properties as it has been shown that there is a relationship between forward scattered light and cell volume and this has become common practice in flow cytometry. Cryobiological conditions induce changes in cells that alter their light scatter properties. Cells with membrane damage from freeze–thaw stress produce lower forward scatter signals and may fall below standard forward scatter thresholds. In contrast to light scatter properties that cannot identify damaged cells from debris, fluorescent dyes used in membrane integrity and mitochondrial polarization assays are capable of labeling and discriminating all cells in suspension. Under cryobiological conditions, isolating cell populations is more effectively accomplished by gating on fluorescence rather than light scatter properties. This study shows the limitations of using forward scatter thresholds in flow cytometry to identify and gate cells after exposure to a freeze–thaw protocol and demonstrates the use of fluorescence as an alternative means of identifying and analyzing cells.

Introduction

Flow cytometry has been shown to be a valuable tool for assessing viability of individual cells in suspension. In flow cytometry, light is scattered by individual cells in a laser beam, and the light scatter properties of these cells distinguish cell populations. In addition, specific wavelengths are analyzed to probe fluorescent emission from surface markers on cells after specific labeling. Different characteristics of cells can influence the pattern of detected scattered light at forward and side angles. Forward light scatter has widely been used as an indicator of cell size as it has been shown that under specific conditions forward light scatter changes in relation to cell volume [16,26,27,43], whereas side scattered light is influenced by nuclear morphology and cytoplasmic granulation reflecting the complexity of the internal structure of cells [6,28]. In analysis of flow cytometry data, the combination of forward and side scatter has been used to identify specific cell types and subpopulations [28,38,48].

Common practice in flow cytometry is to identify and separate cells from background and debris using a trigger, also referred to as the discriminator, that is traditionally based on a forward scatter threshold [8,29], which assumes that forward scattered light correlates with cell or particle volume. However, a study of osmotic stress in hamster fibroblasts, granulocytes, and lymphocytes showed that forward light scatter was inversely proportional to cell volume in anisotonic solutions [24]. The complexity of the cell and its properties suggests that size is not the only factor that affects forward scattered light [14]. Other relevant factors include the wavelength used to generate light scatter signals [19,30], the angle of detection of scattered signals [20,37], differences in the refractive index [39,41], properties of the plasma membrane, and the presence of internal cell structures [25].

Light scatter is not the only option when utilizing a trigger for distinguishing cells; there have also been applications using fluorescence as a method of cell identification in flow cytometry. The fluorescence of nucleic stains and monoclonal antibodies have been combined with light scatter to identify damaged and intact cells in fixed flow cytometric samples [50], and as a variable to

☆ *Statement of funding:* This research was funded by the Canadian Institutes of Health Research (MOP 86492, INO 126778), The Government of Alberta (Graduate Student Scholarship of Advanced Education and Technology) and the University of Alberta (Graduate Research Assistantship). JAW Elliott holds a Canada Research Chair in Thermodynamics.

* Corresponding author at: University of Alberta, Edmonton, AB T6G 2V4, Canada. Fax: +1 780 492 2881.
E-mail address: janet.elliott@ualberta.ca (J.A.W. Elliott).

http://dx.doi.org/10.1016/j.cryobiol.2014.05.009
0011-2240/

separate components of heterogeneous whole blood [49]. A study by Loken et al. [18] showed that in a light scatter distribution, the position of a peak of two attached cells was not double that of the peak for single cells, and this non-additive property was an indication that light scatter was not directly proportional to cell volume. However, in that same study, a fluorescein fluorescence profile of these same cells showed cell doublets emitting twice the fluorescent intensity of single cells [18]. Lu et al. [21] showed that light scatter measurements could not accurately quantify spermatozoa in human sperm cell concentrates. The concept of using fluorescence as a threshold has been previously used in flow cytometry for the purposes of sorting minor subpopulations of cells [23] and for detection of rare events [35]. Fluorescence has also been combined with Coulter counter measurements, revealing size and permeability characteristics of cells and contributing to sorting viable cells from "waste" in suspension [13]. These examples demonstrate that although light scatter is an important parameter in flow cytometry, there are situations where fluorescence may be a more reliable indicator to identify cells.

There is increasing interest in using flow cytometry as a quantitative method of cellular assessment in cryobiological studies [1,4,11]. Cryobiology is the study of biological responses to low temperatures and cryopreservation provides a means of preserving viability and function of cells and tissues for long periods. Assessment of cellular viability is used in cryobiology to measure the quality of individual samples, and optimize protocols to improve cryopreservation outcomes [5]. The plasma membrane is considered a primary site of cryoinjury [22,44], and in cryobiology membrane integrity is one of the most commonly-used methods to determine viability. Assays of plasma membrane integrity are simple, rapid assessments, primarily measured using dye exclusion methods [32], or combinations of fluorescence [2,9,24,46]. Cryopreservation studies have also used membrane integrity assays in conjunction with more specific assessments of cell function to understand cellular responses, including changes in metabolic function [5,31], DNA fragmentation [10], and mitochondrial polarization [47].

Cryobiological conditions induce significant alterations in cellular light scattering properties. A study by McGann et al. [24] exposing cells to cryobiological conditions showed that cooling to low temperatures and freezing cells resulted in low membrane integrity and decreased forward light scatter, under conditions that resulted in only a slight reduction in cell volume. These observations contradict the assumption that the forward light scatter is proportional to volume [17], and suggested that other properties of the cell surface and the cytoplasm may also contribute to the light scatter of cells [24].

The objective of this study was to demonstrate that gating strategies based on forward light scattering may introduce inaccuracies in experiments that require the identification of total cell populations, including not only live, but also dead and damaged cells. This study also investigated the use of fluorescence-based gating as an alternative strategy to identify all cells in a sample population.

Materials and methods

Cell cultures

mm?>Human umbilical vein endothelial cells (HUVEC) (Lot#0000120825; Lonza®, Walkersville, MD, USA) were cultured at 37 °C and 5% CO_2 in endothelial basal media (EBM-2) supplemented with a bullet kit (Lonza®) containing human fibroblast growth factor B, hydrocortisone, vascular endothelial growth factor, ascorbic acid, heparin, human endothelial growth factor, and fetal bovine serum. For cell passage, cultures were incubated to approximately 40% confluence within the culture flask, according to LONZA guidelines. For experiments, cultures were incubated to approximately 50% confluence then harvested by exposure to trypsin–EDTA (Lonza®) for 2 min at 37 °C. Cell suspensions were centrifuged at 201*g* for 5 min in a 5810R tabletop centrifuge (Eppendorf, Westbury, NY, USA), and resuspended in endothelial growth media at a concentration of 1.0×10^6 cells/mL in 1 mL aliquots maintained in 12×75 mm round bottom plastic tubes (VWR, Edmonton Canada) prior to experimentation.

Membrane integrity assessment of cell recovery

The dual fluorescent assay (SytoEB) uses a combination of two fluorescent dyes, Syto13 (Molecular Probes, Eugene, OR, USA) and ethidium bromide (EB) (Sigma–Aldrich, Mississauga, ON, Canada) to assess cell membrane integrity. Syto13 is a DNA/RNA binding stain that permeates all cells and fluoresces green on excitation by UV wavelengths. Ethidium bromide permeates cells with damaged plasma membranes, exhibiting red fluorescence upon UV exposure. The combination of these two dyes makes a binary assay with membrane intact cells exhibiting green fluorescence (Syto13) and membrane compromised cells exhibiting red fluorescence (EB). The SytoEB stain was prepared using 1× phosphate buffered saline (PBS), and aliquots of Syto and EB diluted from the stock solution. The final dye was comprised of 25 μM EB and 12.5 μM Syto13. 10 μL of the prepared dye were added to the 1 mL aliquot of HUVEC in suspension and incubated for 2 min at room temperature before analysis.

Mitochondrial membrane potential assessment of cell recovery

The ratiometric dye 5′,6,6′-tetrachloro-1,1′,3,3′-tetraethylbenzimidazolylcarbocyanine-iodide (JC-1) (Molecular Probes, Eugene, OR, USA) was used as an indicator of mitochondrial membrane potential of HUVEC in suspension. The fluorescence shifts from green (~525 nm) in low polarization states (non-functional mitochondria) to red (~590 nm) in high polarization states (functioning mitochondria). This change in color of fluorescence is based on a concentration-dependent shift from monomers of the dye which fluoresce green to J-aggregates which fluoresce red [34]. Initially the dye is present as cationic monomers (green) that permeate into cells, influenced by the negative intracellular potential. In healthy cells these monomers permeate into the mitochondrial matrix, drawn by the electronegative interior of mitochondria where these monomers form J-aggregates (red) [15]. Therefore cells with depolarized mitochondria predominately emit green fluorescence from monomers present in the cytoplasm, and cells with polarized mitochondria predominantly emit red fluorescence from J-aggregates of the dye.

The JC-1 assay was prepared from a stock solution made by combining 5 mg of the JC-1 reagent with 5 mL of DMSO (Sigma–Aldrich) to a concentration of 1 mg/mL. 0.8 μL of JC-1 reagent/DMSO solution was added to 0.4 mL aliquots of HUVEC (final concentration of 2 μg/mL) and incubated for 30 min in the incubator at 37 °C and 5% CO_2.

Cell treatment conditions

Control group

The first group of cells was left for 5 min at room temperature after staining, prior to analysis for flow cytometry.

Mitochondrial depolarization group

Tubes from the second group (CCCP samples) were treated with the mitochondrial depolarization reagent carbonyl cyanide 3-chlorophenylhydrazone (CCCP). The CCCP samples were created by preparing a 5 mM working concentration of the CCCP reagent

(Sigma–Aldrich) in DMSO. Four microliters of CCCP/DMSO solution were added to the 0.4 mL cell suspension (50 μM final concentration) and incubated simultaneously with the JC-1 reagent for 30 min prior to flow cytometry analysis.

The CCCP reagent was dissolved in DMSO (>99.9%); 4 μL of DMSO is present in the 0.4 mL cell sample, giving a final concentration of approximately 1%. An even smaller concentration of DMSO results with the use of the JC-1 reagent. Although this compound is commonly used in procedures for its cryoprotective properties, the concentrations used in this investigation are too low to induce any significant cryoprotective effect.

Plunged group

Tubes from the third group were plunged directly into liquid nitrogen for 2 min, and then subsequently thawed in a 37 °C water bath until no visible ice was present. This group was considered a control for dead cells, emphasizing the extent of cryoinjury that could be induced during cryopreservation procedures. After thawing, these cells were then stained prior to analysis with the flow cytometer.

Flow cytometry analysis

Cell aliquots were assessed with an unmodified Coulter® EPICS® XL-MCL™ flow cytometer (Beckman-Coulter) equipped with a 488 nm argon laser. Emission of Syto13 and JC-1 monomers was detected using the FL1 (505–545 nm) bandpass filter; emission of JC-1 aggregates was detected using the FL2 (560–590 nm) bandpass filter, and emission of ethidium bromide was detected using the FL3 (605–635 nm) bandpass filter. Aliquots of HUVEC (0.4 mL) were loaded and run for a time interval of 2 min in Isoflow™ sheath fluid (Beckman-Coulter).

Fluorescence compensation and data acquisition were performed using System II™ software (Beckman-Coulter). Fluorescence compensation for the membrane integrity assay (SytoEB) was achieved by subtracting 27.5% of FL1 (Syto13) from FL3 (EB), whereas compensation for the mitochondrial membrane potential was achieved by subtracting 43% FL1 (JC-1 green) from FL2 (JC-1 red). The corresponding compensated data was analyzed with the Kaluza® v1.2 flow cytometry analysis software (Beckman Coulter), producing one and two parameter histograms of both the light scatter and fluorescent properties for each sample.

The guidelines used to set fluorescence compensation are found in the text "Practical Flow Cytometry, 4th Ed." [40]. For membrane integrity, two fluorescent stains were used, and for mitochondrial polarization a single two-color stain was used, and thus, two-color compensation of spectral overlap could be achieved simply by subtracting the signals on a linear scale for each detector. Compensation was first performed with manual adjustments on the instrument itself and then double checked using the software "Kaluza v1.2" from the manufacturer Beckman-Coulter.

Fluorescence compensation was conducted individually for each type of experiment, once for membrane integrity (using Syto13 and ethidium bromide) and again for mitochondrial polarization (JC-1). However, the settings of fluorescence compensation were kept the same for each run throughout each experiment. It should be noted that the compensation conditions stated in the manuscript are specific to the fluorescent stains and instrumentation used in the investigation.

The flow cytometer used in the investigation was subject to routine quality control runs in order to ensure accuracy of results. The instrument underwent routine monthly checks carried out using fluorescent beads purchased from the manufacturer.

This research article meets the minimum information standard for flow cytometry experiments (MIFlowCyt). The raw flow cytometry data is available in the Flow Repository (www.flowrepository.org – ID: FR-FCM-ZZ6W).

Results

Effectiveness of forward light scatter gating

Fig. 1 shows typical light scatterplots of the forward scatter (*y*-axis) and side scatter (*x*-axis) of HUVEC in suspension, either untreated HUVEC control, or after cells have been plunged into liquid nitrogen. Each dot on these plots represent a single event through the flow cytometer. Fig. 1A shows the raw unprocessed data of all events in room temperature controls, and depicts three populations, grouped into regions: R1 with high forward and high side scatter events (26%), R2 with low forward and high side scatter events (6%), and R3 with low forward and low side scatter events (68%). Commonly, a threshold is established on the forward scatter channel under the assumption that this threshold allows for the discrimination of cells from debris, where only events greater than the value of this threshold will be registered by the flow cytometer. Fig. 1B shows the same data as Fig. 1A, after application of a threshold on the forward scatter intensity, where events with forward scatter intensity below the threshold have been removed. Though debris makes up the majority of events in R3, this is not necessarily true for the events in R2. Fig. 1C shows a plot of forward versus side scatter for HUVEC without cryoprotectant directly plunged into liquid nitrogen to induce cryoinjury including the raw unprocessed data of all events. In Fig. 1C two populations R2 (32%) and R3 (68%) consist of the majority of events, with few events present in R1 (<1%). Fig. 1D shows the data after application of the forward scatter threshold, where the applied threshold now excludes the majority of events.

A comparison of Fig. 1A (control) and C (plunged) shows that the number of events in R1 has decreased and the number in R2 has increased, indicating that the events of R1 have moved to R2 after plunging these cells into liquid nitrogen. This implies that events from R1 represent healthy cells, whereas events from R2 represent damaged cells. In the untreated control (Fig. 1A), there are some events present in R2 (6% of total events). Identifying these events as damaged cells indicates that they make up approximately 19% of total cells present; this is similar to our observations using fluorescence microscopy, as approximately 15–20% of cells were found to be membrane damaged in control cell populations of freshly trypsinized HUVEC in suspension (data not shown). Applying the typical forward scatter threshold to Fig. 1D (plunged) removes these damaged cells, excluding them from further analysis.

Effectiveness of fluorescence gating with a membrane integrity assay – SytoEB

Fig. 2 shows a membrane integrity analysis performed using flow cytometry of HUVEC stained with fluorescent dyes Syto13 and EB, showing analysis of both HUVEC control samples (Fig. 2A–C) and HUVEC plunged into liquid nitrogen (Fig. 2D–F). Fig. 2A and D show histograms of green fluorescence (Syto13: a dye that enters all cells), and Fig. 2B and E show histograms of red fluorescence (EB: a dye that permeates only membrane damaged cells). Histograms show a peak of low fluorescence events separated from a peak of highly fluorescent events. Because Syto13 and EB have a high yield of fluorescence when bound to nucleic acids [45,51], it is reasonable to conclude that the low intensity peaks represent debris and high intensity peaks represent cells. Thresholds were placed at the minima between the peaks of events to separate the low green from high green regions (Fig. 2A and D)

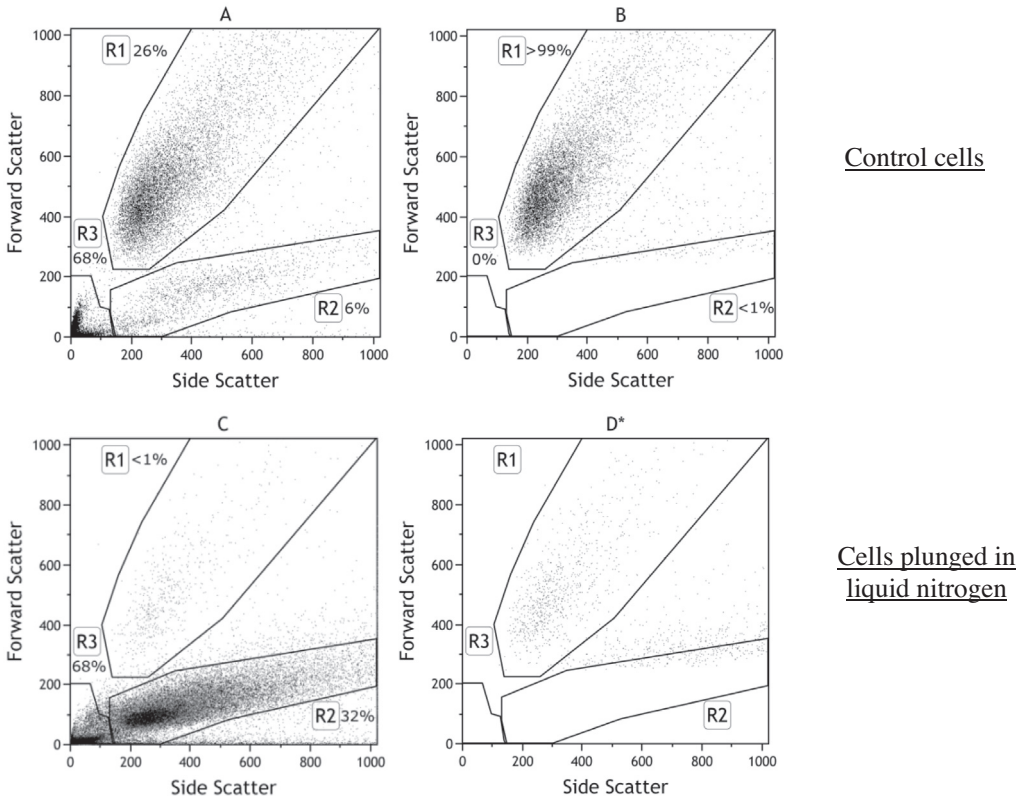

Fig. 1. Flow cytometry forward vs. side scatter intensity plots of HUVEC. (A) Raw data showing all events in room temperature controls. (B) Data after application of a threshold on the forward scatter intensity in room temperature controls. (C) Raw data showing all events after plunging in liquid nitrogen. (D) Data after application of a threshold on the forward scatter intensity after plunging in liquid nitrogen. *Percentages excluded due to the low number of total events registered by the flow cytometer.

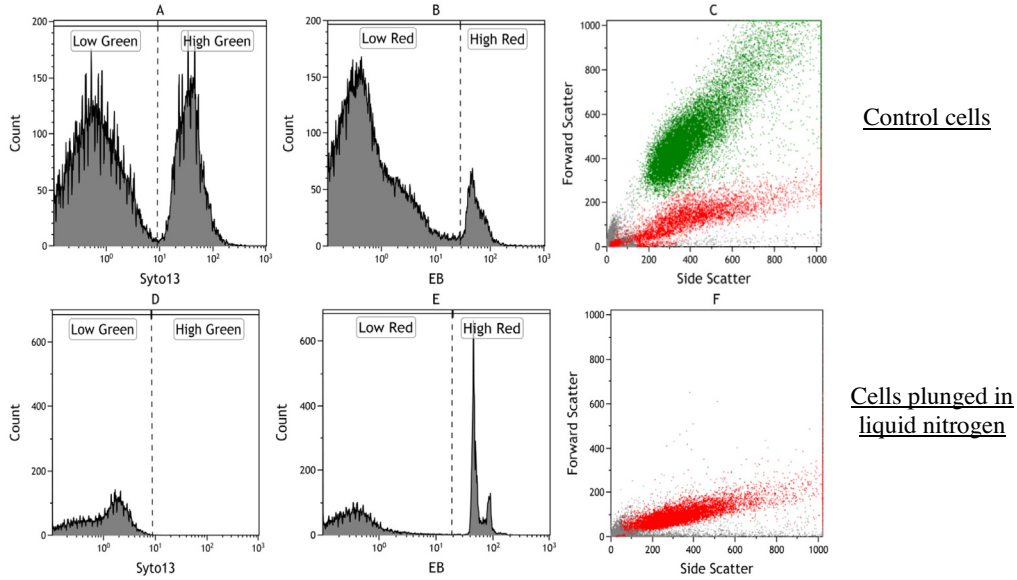

Fig. 2. SytoEB membrane integrity analysis of HUVEC as measured by flow cytometry. (A) Histogram of Syto13 fluorescence intensity in control samples. (B) Histogram of ethidium bromide fluorescence intensity in control samples. (C) Forward versus side scatter showing segregation of membrane intact cells (green), membrane compromised cells (red), and debris (grey) in control samples. (D) Histogram of Syto13 fluorescence intensity in plunged samples. (E) Histogram of ethidium bromide fluorescence intensity in plunged samples. (F) Forward versus side scatter showing segregation of membrane intact cells (green), membrane compromised cells (red), and debris (grey) in plunged samples.

as well as low red from high red regions (Fig. 2B and E). For both dyes this threshold was placed to identify events as cells (high green and high red) from debris (low green and low red) with the dyes identifying the membrane integrity of those cells as membrane intact (high green), or membrane damaged (high red).

A closer look at Fig. 2D shows a histogram of the green fluorescence raw data with a peak present in the low green region, but no peak in the high green region, indicating that there are almost no membrane intact cells after plunging cells in liquid nitrogen. Fig. 2E shows a low intensity peak in the low red region, and a high

intensity peak in the high red region. Comparing the control sample (Fig. 2A and B), with the plunged sample and (Fig. 2D and E), shows the number of intact cells that become damaged when plunged into liquid nitrogen, represented here by a shift from green to red fluorescence. The thresholds based on membrane integrity fluorescent dyes are able to distinguish both intact control cells and cells damaged by cryoinjury from debris, which is impossible using a traditional forward scatter threshold.

Fig. 2C and F show the raw forward versus side scatter data of HUVEC control and plunged samples, respectively, showing cells with high intensity Syto13 events (green), high intensity EB events (red), and the remaining events in grey, indicating that membrane intact cells (green) and membrane compromised cells (red) could be distinguished from debris (grey). In Fig. 2C, the membrane intact cells make up approximately 82% of total cells and also match the cell population in R1 (Fig. 1A), whereas membrane compromised cells make up approximately 18% of the total cells and match the cell population in R2 (Fig. 1A), further indicating that R1 and R2 are comprised of healthy and damaged cells respectively. It is noted that there is a proportion of cells (red events, Fig. 2C) that are present in region R3 (Fig. 1). These red fluorescent events are an indication that damaged cells with low light scatter properties may be present in R3. Alternatively, these events may be due to the presence of cell particulate or microparticles from microvesiculation of cells, an occurrence that is observed during long-term storage of red blood cells [3,7,12].

Fig. 3 shows the events registered by the flow cytometer that have been identified as cells when using either a light scatter, or a fluorescence threshold. The multiparameter capability of the flow cytometer allows for direct comparison of the light scatter and fluorescence properties of each recorded event. A comparison of the two gating strategies for HUVEC controls shows a similar number of healthy cells gated by either light scatter or fluorescence. Using fluorescence gates, an increase was observed in the number of damaged cells (EB) in plunged samples compared to controls. However, the light scatter threshold excludes many damaged cells from both control and plunged samples. The total number of cells observed using light scatter gates was approximately 60% less than the total number observed using fluorescence gates, indicating that light scatter thresholds are ineffective at detecting damaged cells in both control and plunged samples whereas fluorescence gating allows for detection of most cells in the suspension.

Effectiveness of fluorescence gating with a mitochondrial polarization assay – JC-1

JC-1 was used as an indicator of mitochondrial polarization to identify healthy and cryoinjured cells from debris. Fig. 4A and B show JC-1 green fluorescence of HUVEC control samples. Fig. 4A shows a fluorescence histogram separating low intensity events

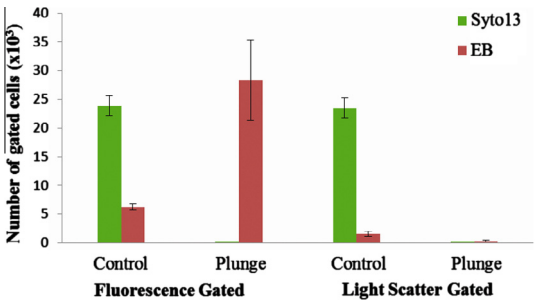

Fig. 3. Membrane integrity analysis of events identified as cells using Syto13 (green) and ethidium bromide (red) in HUVEC control and plunge samples with either light scatter or fluorescence gates (mean ± sem; $n = 3$).

(low green), from high intensity events (high green). High intensity events correspond to the cell population, whereas low intensity events represent debris in suspension, elucidated by the action of the JC-1 assay, a membrane potential dependent stain that requires a negatively charged intracellular environment in order for its monomers to concentrate. By establishing a threshold between the low-green and high-green regions based on the fluorescent intensity of JC-1 monomers, the cell population of interest is now easily distinguished from debris for further analysis.

A closer look at the high green region in Fig. 4A shows two peaks present: a lower intensity peak with a high percentage of high-green cell events (peak 1: 75.8 ± 2.0%), and a higher intensity peak with a low percentage of high-green cell events (peak 2: 24.6 ± 2.0%). Since the green fluorescence intensity of JC-1 depends on the concentration of monomers, lower intensity events (peak 1, Fig. 4A), and higher intensity events (peak 2, Fig. 4A), with both being in the high-green region corresponding to cells, will depict cells with polarized and depolarized mitochondria respectively.

Fig. 4B show the raw forward versus side scatter data of HUVEC control samples after the application of this fluorescence threshold with cells containing polarized (green) and depolarized mitochondria (orange) clearly distinguished from debris (grey). Cells with polarized mitochondria (green, Fig. 4B), show similar light scatter properties to membrane intact cells (green, Fig. 2C). Correspondingly, cells with depolarized mitochondria (orange, Fig. 4B), show similar light scatter properties to membrane compromised cells (red, Fig. 2C). This provides further evidence of the accuracy of fluorescence thresholds, as two separate assays were capable of not only discriminating cells from debris but also identifying intact from damaged cells.

Fig. 4C shows the JC-1 green fluorescence of HUVEC samples with the addition of the mitochondrial depolarization agent CCCP, used as a negative control for mitochondrial membrane potential without affecting the membrane integrity of the cell. Fig. 4C shows a fluorescence histogram separating low fluorescent intensity debris (low green) from high intensity cells (high green). Even after depolarization of mitochondria in all cells within the sample from incubation with CCCP, these cells were still readily identified from debris using a fluorescence threshold at the minimum between the low green and high green regions. A comparison of JC-1 green fluorescence shows only one peak present in the high green region (Fig. 4C), compared to the two peaks present in control samples (Fig. 4A).

Fig. 4D shows the forward versus side scatter data of HUVEC samples after the application of a fluorescence threshold, identifying cells with depolarized mitochondria (orange) from debris (grey). Although the fluorescent properties of cells have changed (Fig. 4C), compared to untreated controls (Fig. 4A), the light scatter properties of both of these samples remain the same (Fig. 4B and D). A large population of cells with high forward and side scatter properties is still present along with a smaller population of cells with low forward and high side scatter corresponding to the events found in R1 and R2 (Fig. 1A), respectively.

Fig. 4E and F show the JC-1 green fluorescence of HUVEC plunged samples. Fig. 4E shows a fluorescence histogram separating low intensity debris (low green), from high intensity cells (high green). A comparison of fluorescent intensity (peak intensity expressed in units from the flow cytometer: au) showed that cells (high green) had increased fluorescence in plunged samples (54.8 ± 1.4 au, Fig. 4E), compared to controls (21.1 ± 0.6 au, Fig. 4A). The lower intensity of green fluorescence in controls (high green, Fig. 4A), is due to the lack of JC-1 monomers present in cells, as under control conditions monomers form aggregates in mitochondria and fluoresce red, lowering the overall intensity of green fluorescence, indicating healthy living cells [42]. The higher peak of fluorescent intensity (high green, Fig. 4E) shows damaged cells

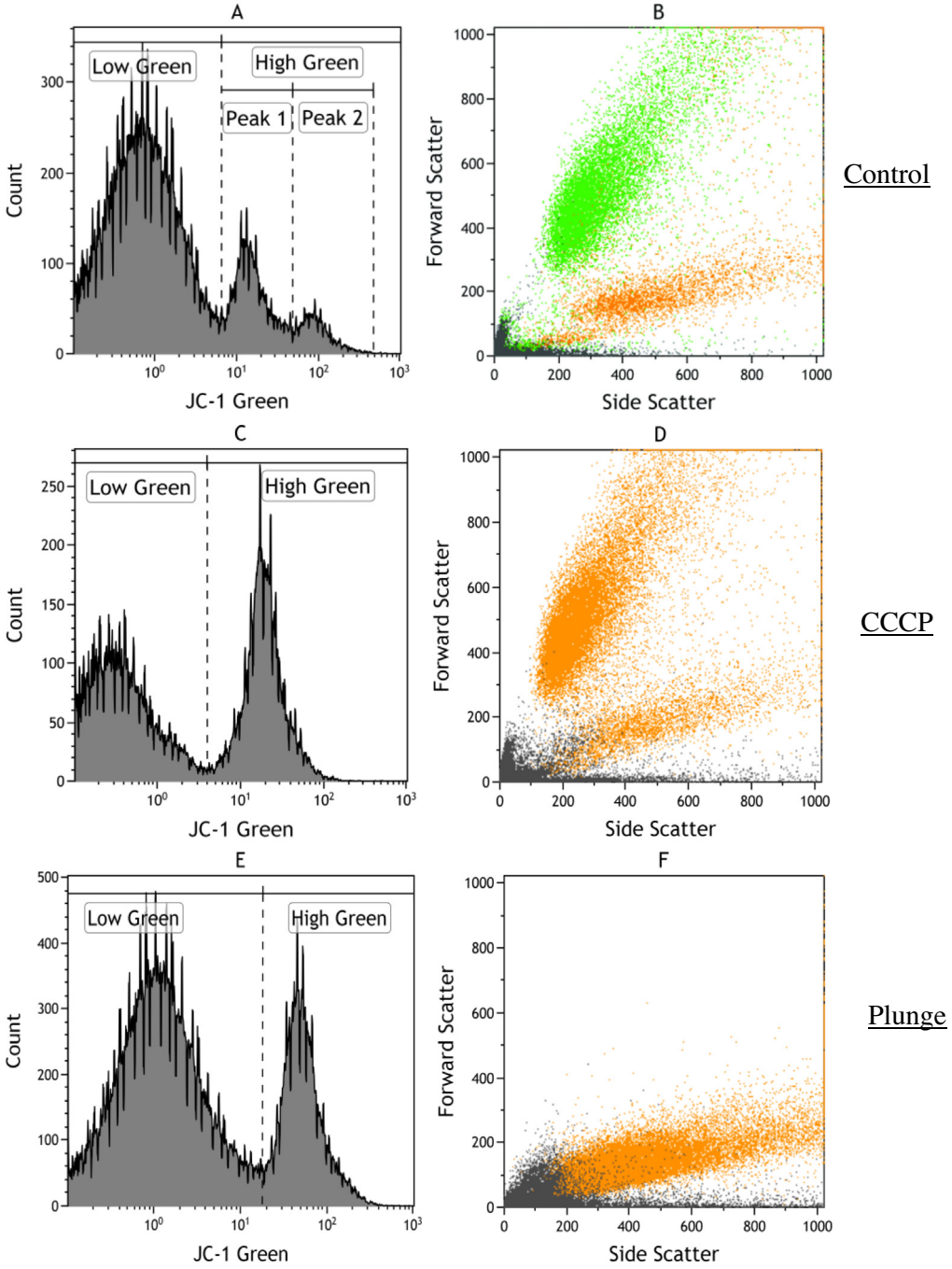

Fig. 4. JC-1 mitochondrial polarization analysis of events gated as cells and debris in HUVEC measured with flow cytometry. (A) Histogram of JC-1 green fluorescence intensity showing cells (high green) with polarized (peak 1) and depolarized (peak 2) mitochondria separate from debris (low green) in controls samples. (B) Forward versus side scatterplot showing identification of cells with polarized (light green) and depolarized (orange) mitochondria from debris (grey) in control samples. (C) Histogram of JC-1 green fluorescence intensity in control samples with the addition of CCCP. (D) Forward versus side scatter plot showing segregation of cells (orange) from debris (grey) in control samples with the addition of CCCP. (E) Histogram of JC-1 green fluorescence intensity in plunged samples. (F) Forward versus side scatter plot showing segregation of damaged cells (orange) from debris (grey) in plunged samples.

with depolarized mitochondria. Fig. 4A and B along with Fig. 4E and F show that intact and damaged mitochondria are accurately distinguished from debris with a fluorescence threshold.

The mitochondrial membrane potential of events identified as cells (from Fig. 4) were also assessed using a one parameter histogram of the intensity of red fluorescence. The red fluorescence intensity of J-aggregates from the mitochondrial polarization assay JC-1 and the corresponding light scatter properties of HUVEC are presented in Fig. 5. The forward and side light scatter properties of control (Fig. 5A), and plunged (Fig. 5B), samples are presented with a corresponding histogram of JC-1 red fluorescence (Fig. 5C). The high red fluorescence in control cells (red peak, Fig. 5C), is from the formation of J-aggregates present in cells with polarized mitochondria, whereas the low red fluorescence of plunged cells (blue peak, Fig. 5C), occurs when mitochondria are depolarized. Cells with high red fluorescence and corresponding high forward and high side scatter properties indicate cells with intact mitochondria (red) and cells with low red fluorescence and low forward scatter

properties indicate cells with damaged mitochondria (blue). JC-1 not only discriminates cells from debris but also reflects the functional capacity of HUVEC based on the polarized state of their mitochondria indicated by the presence of red fluorescent J-aggregates.

Discussion

Light scatter is used as a key parameter in flow cytometry to reveal information about cell size and morphological characteristics that can aid in the identification of cell types and subpopulations; however the relationship between light and particle properties is complex. Since Mullaney et al. demonstrated a relationship between forward light scatter and cell volume under the assumption that cells were homogenous spheres with a uniform refractive index [27] a common generalization has emerged that light scatter in the forward direction gives an estimation of cell size. Though volume does play a major role, there are limitations to this generalization, and it has been shown that with polystyrene latex microspheres forward scattered light increases with diameter in a non-linear manner [39], indicating that other factors are also involved. It is obvious that cells are not merely spheres with set diameters and refractive indices whose behavior is unaltered by a changing environment. These factors introduce limitations to using forward scattered light as a trigger to discriminate cells from background and debris under some conditions. The non-specific binding of antibodies in immunofluorescence studies to dead and damaged cells was problematic when trying to distinguish intact cells of interest, especially in samples containing different cell types; using a forward scatter threshold to distinguish cells was the simplest means of reducing artifacts from this non-specific binding. The application of this threshold to HUVEC room temperature controls shows how easily intact cells are identified from debris (Fig. 1B).

In cryobiological studies that require numeration of both damaged and healthy cells during assessments, traditional use of a light scatter threshold would lead to the exclusion of damaged cells of interest. These investigations often use the ratio of healthy to total cells (healthy and damaged) to determine the effectiveness of cryopreservation protocols. Plunging HUVEC directly into liquid nitrogen shows the extent of damage that can occur to cells in a cryopreservation procedure and the ineffectiveness of the forward scatter threshold to discriminate between debris, damaged cells and healthy cells (Fig. 1D). For cryobiological studies that need to include damaged cells in the final assessment, an alternative strategy of gating and discriminating cells is required.

The plasma membrane which has been shown to be a contributing factor to light scatter characteristics of cells is also an important determinant of cell viability. Under cryobiological conditions the membrane acts as a barrier to ice propagation during freezing, and is believed to be one of the primary sites of cryoinjury during exposure to freeze–thaw stress [33,44]. The plasma membrane is an ideal candidate to test the effectiveness of light scatter and fluorescence gating strategies to discriminate healthy and damaged cells from debris. A fluorescent membrane integrity assay (SytoEB) was used to assess the state of the cell membrane in HUVEC room temperature controls and HUVEC plunged into liquid nitrogen (Fig. 2).

The nucleic acid staining dyes of the membrane integrity assay (SytoEB) demonstrate the versatility of fluorescence measurements as membrane intact cells have high forward scatter and high green fluorescence, whereas damaged cells have low forward scatter and high red fluorescence. Due to the similarities in forward light scatter of damaged cells and debris it is difficult to accurately distinguish damaged cells from debris using forward light scatter alone. In cryobiological studies where the proportion of damaged to total (intact and damaged) cells is to be used; discarding damaged cells from assessment would introduce bias in the final result (Fig. 3). The use of fluorescence intensity gives a more accurate measure for viability and a comparison of control and plunged HUVEC samples shows the advantage of using fluorescence over light scatter based thresholds in cryobiological applications (Fig. 3).

Fluorescent assays are not limited to assessments of the plasma membrane; there is the capability of probing other cellular characteristics. The JC-1 fluorescent dye is an indicator of mitochondrial membrane polarization from its formation of red–orange fluorescent J-aggregates [42]. In control samples the high green region (high green, Fig. 4A), shows cells with a higher intensity of green fluorescence than the extraneous events in suspension (low green, Fig. 4A), indicating that not all monomers of the dye form J-aggregates in healthy cells and that a number of green fluorescent monomers remain in the cell cytoplasm.

A closer observation of control JC-1 fluorescence shows two peaks, a first peak indicating cells with high forward scatter properties, and a second peak of cells with low forward scatter, further confirming our use of fluorescence to discriminate between healthy and damaged cells (high green, Fig. 4A). When looking at HUVEC treated with CCCP a different picture emerges; only one peak is present indicating depolarization of cell mitochondria but with no alteration in light scatter properties (Fig. 4C and D); an indication that light scatter does not readily distinguish cells that have undergone mitochondrial depolarization, unlike plunged samples that show changes in both fluorescence and light scatter

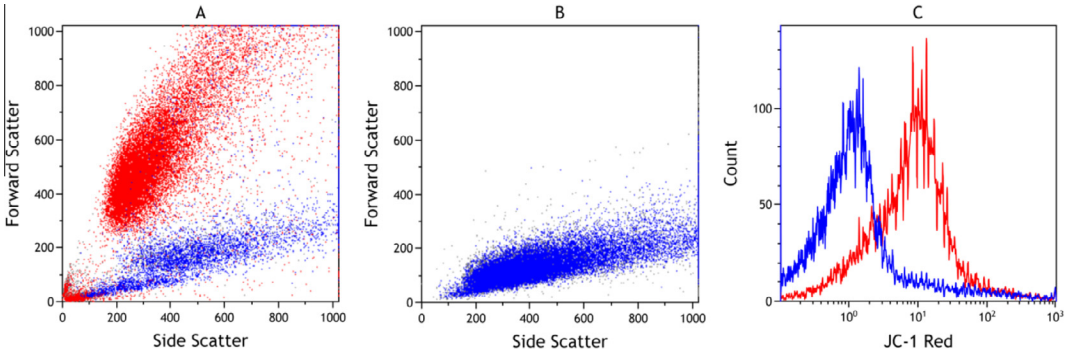

Fig. 5. JC-1 mitochondrial polarization analysis of HUVEC measured with flow cytometry. (A) Forward versus side scatter plot of control cells at room temperature showing cells with polarized (red) and depolarized (blue) mitochondria. (B) Forward versus side scatter plot of cells plunged directly into liquid nitrogen showing only cells with depolarized mitochondria (blue). (C) Histogram comparing the intensity of red fluorescence of control (red) and plunged (blue) cells.

properties (Fig. 4E and F). Despite the differences in the fluorescent mechanism of a mitochondrial polarization assay compared to a membrane integrity assay, the same result was attained, further reinforcing the versatility of fluorescence based cell discrimination.

In addition to discriminating cells, JC-1 also gives an indication of the functional state of mitochondria based on the intensity of red fluorescent JC-1 aggregates. The polarized state of mitochondria in control samples gave off higher intensity of fluorescence when compared to plunged cells (Fig. 5). JC-1 has been found useful as a ratiometric assay, as healthy cells primarily give off high red and low green fluorescence, whereas damaged cells give off low red and high green fluorescence; this ratio may be used to determine the polarization state of mitochondria in cells [36].

Conclusions

In this study the effectiveness of using light scatter and fluorescence gating strategies in flow cytometry for cryobiological applications were compared. These strategies were used to identify HUVEC from debris in control samples and in samples that had been plunged directly into liquid nitrogen. The traditional method of using forward scattered light as a trigger signal to discriminate cells excluded the majority of cryoinjured cells from assessment along with debris. Though this is not a concern when conducting studies with immunofluorescence, it is problematic for studies that need to take into account the proportion of viable to total (viable and non-viable) cells such as in cryobiology. An alternative to forward light scatter is to use the fluorescence signal intensity to discriminate both healthy and damaged cells from debris.

In addition to these findings this study also showed that HUVEC control and cryoinjured cells were effectively identified under control and plunged conditions using fluorescence assessments of membrane integrity, a commonly used assessment of cell viability, and mitochondrial polarization an indicator of the functional state of cellular mitochondria. A common nucleic acid based membrane integrity assay such as the combination of Syto13 and ethidium bromide easily identifies as cells those events with high intensity fluorescent signals. The JC-1 dye not only discriminated cells from background and debris based on the intensity of green JC-1 monomers but in addition also indicated the functional state of cellular mitochondria. These assays demonstrate that fluorescent stains of very different mechanisms can be equally effective at identifying healthy and damaged cells with the flow cytometer under conditions where light scatter has shown to be unreliable. Flow cytometry can be a valuable tool in studies involving cryo-damage as long as the limitations of traditional methods are taken into account, and the alternatives are considered.

Acknowledgments

This research was funded by the Canadian Institutes of Health Research (MOP 86492, INO 126778), the Government of Alberta (Graduate Student Scholarship of Advanced Education and Technology) and the University of Alberta (Graduate Research Assistantship). JAW Elliott holds a Canada Research Chair in Thermodynamics.

References

[1] J.F. Abrahamsen, A.M. Bakken, Ø. Brusserud, B.T. Gjertsen, Flow cytometric measurement of apoptosis and necrosis in cryopreserved PBPC concentrates from patients with malignant diseases, Bone Marrow Transplant. 29 (2002) 165–171.
[2] J.P. Acker, L.E. McGann, Cell–cell contact affects membrane integrity after intracellular freezing, Cryobiology 40 (2000) 54–63.
[3] R. Almizraq, J.D. Tchir, J.L. Holovati, J.P. Acker, Storage of red blood cells affects membrane composition, microvesiculation, and in vitro quality, Transfusion 53 (2013) 2258–2267.
[4] B. Balint, D. Paunovic, D. Vucetic, D. Vojvodic, M. Petakov, M. Trkuljic, N. Stojanovic, Controlled-rate versus uncontrolled-rate freezing as predictors for platelet cryopreservation efficacy, Transfusion 46 (2006) 230–235.
[5] J. Baust, R. Van Buskirk, J. Baust, Cell viability improves following inhibition of cryopreservation-induced apoptosis, In Vitro Cell. Dev. Biol. Anim. 36 (2000) 262–270.
[6] M.C. Benson, D.C. McDougal, D.S. Coffey, The application of perpendicular and forward light scatter to assess nuclear and cellular morphology, Cytometry 5 (1984) 515–522.
[7] B. Bicalho, J.L. Holovati, J.P. Acker, Phospholipidomics reveals differences in glycerophosphoserine profiles of hypothermically stored red blood cells and microvesicles, Biochim. Biophys. Acta 2013 (1828) 317–326.
[8] G. Boeck, Current status of flow cytometry in cell and molecular biology, Int. Rev. Cytol. 204 (2001) 239–298.
[9] F. Dankberg, M.C. Persidsky, A test of granulocyte membrane integrity and phagocytic function, Cryobiology 13 (1976) 430–432.
[10] T.M. Gliozzi, L. Zaniboni, S. Cerolini, DNA fragmentation in chicken spermatozoa during cryopreservation, Theriogenology 75 (2011) 1613–1622.
[11] M. Hagedorn, J. Ricker, M. McCarthy, S.A. Meyers, T.R. Tiersch, Z.M. Varga, F.W. Kleinhans, Biophysics of zebrafish (*Danio rerio*) sperm, Cryobiology 58 (2009) 12–19.
[12] J.L. Holovati, K.A. Wong, J.M. Webster, J.P. Acker, The effects of cryopreservation on red blood cell microvesiculation, phosphatidylserine externalization, and CD47 expression, Transfusion 48 (2008) 1658–1668.
[13] I.I. Katkov, Taste of the waste: simultaneous electrical cell sizing and flow cytometry (Cell Lab Quanta) clearly separates viable cells from noise, debris, dead cells and clusters, Cryobiology 62 (2011) 88–89.
[14] M. Kerker, Elastic and inelastic light scattering in flow cytometry, Cytometry 4 (1983) 1–10.
[15] G. Kroemer, N. Zamzami, S. Susin, Mitochondrial control of apoptosis, Immunol. Today 18 (1997) 44–51.
[16] P. Latimer, Light scattering vs. microscopy for measuring average cell size and shape, Biophys. J. 27 (1979) 117–126.
[17] P. Latimer, B.E. Pyle, Light scattering at various angles. Theoretical predictions of the effects of particle volume changes, Biophys. J. 12 (1972) 764–773.
[18] M.R. Loken, L.A. Herzenberg, Analysis of cell populations with a fluorescence activated cell sorter, Ann. N. Y. Acad. Sci. 254 (1975) 163–171.
[19] M.R. Loken, D.W. Houck, Light scattered at two wavelengths can discriminate viable lymphoid cell populations on a fluorescence-activated cell sorter, J. Histochem. Cytochem. 29 (1981) 609–615.
[20] M.R. Loken, R.G. Sweet, L.A. Herzenberg, Cell discrimination by multiangle light scattering, J. Histochem. Cytochem. 24 (1976) 284–291.
[21] J.C. Lu, F. Chen, H.R. Xu, Y.M. Wu, X.Y. Xia, Y.F. Huang, N.Q. Lu, Is flow cytometry really adapted to the determination of sperm concentration?, Scand J. Clin. Lab. Invest. 67 (2007) 394–401.
[22] P. Mazur, The role of cell membranes in the freezing of yeast and other single cells, Ann. N. Y. Acad. Sci. 125 (1965) 658–676.
[23] J.P. McCoy Jr., W.H. Chambers, R. Lakomy, J.A. Campbell, C.C. Stewart, Sorting minor subpopulations of cells: use of fluorescence as the triggering signal, Cytometry 12 (1991) 268–274.
[24] L.E. McGann, M.L. Walterson, L.M. Hogg, Light scattering and cell volumes in osmotically stressed and frozen–thawed cells, Cytometry 9 (1988) 33–38.
[25] R.A. Meyer, A. Brunsting, Light scattering from nucleated biological cells, Biophys. J. 15 (1975) 191–203.
[26] P.F. Mullaney, M.A. Van Dilla, J.R. Coulter, P.N. Dean, Cell sizing: a light scattering photometer for rapid volume determination, Rev. Sci. Instrum. 40 (1969) 1029–1032.
[27] P. Mullaney, P. Dean, Small angle light scattering of biological cells – theoretical considerations, Biophys. J. 10 (1970) 764–772.
[28] O. Nielsen, J.K. Larsen, I.J. Christensen, A. Lernmark, Flow sorting of mouse pancreatic B cells by forward and orthogonal light scattering, Cytometry 3 (1982) 177–181.
[29] M.G. Ormerod, Flow Cytometry: A Practical Approach, 3rd ed., Oxford University Press, Oxford, New York, 2000, pp. 15–16.
[30] G.R. Otten, M.R. Loken, Two color light scattering identifies physical differences between lymphocyte subpopulations, Cytometry 3 (1982) 182–187.
[31] J. Pasch, A. Schiefer, I. Heschel, N. Dimoudis, G. Rau, Variation of the HES concentration for the cryopreservation of keratinocytes in suspensions and in monolayers, Cryobiology 41 (2000) 89–96.
[32] J. Pasch, A. Schiefer, I. Heschel, G. Rau, Cryopreservation of keratinocytes in a monolayer, Cryobiology 39 (1999) 158–168.
[33] V. Ragoonanan, A. Hubel, A. Aksan, Response of the cell membrane–cytoskeleton complex to osmotic and freeze/thaw stresses, Cryobiology 61 (2010) 335–344.
[34] M. Reers, J-aggregate formation of a carbocyanine as a quantitative fluorescent indicator of membrane potential, Biochemistry 30 (1991) 4480–4486.
[35] M.A. Rehse, S. Corpuz, S. Heimfeld, M. Minie, D. Yachimiak, Use of fluorescence threshold triggering and high-speed flow cytometry for rare event detection, Commun. Clin. Cytometry 22 (1995) 317–322.
[36] S. Salvioli, A. Ardizzoni, C. Franceschi, A. Cossarizza, JC-1, but not DiOC6(3) or rhodamine 123, is a reliable fluorescent probe to assess $\Delta\Psi$ changes in intact cells: implications for studies on mitochondrial functionality during apoptosis, FEBS Lett. 411 (1997) 77–82.
[37] G.C. Salzman, J.M. Crowell, C.A. Goad, A flow system multiangle light scattering instrument for cell characterization, Clin. Chem. 21 (1975) 1297–1304.

[38] G.C. Salzman, J.M. Crowell, J.C. Martin, Cell classification by laser light scattering: identification and separation of unstained leukocytes, Acta Cytol. 19 (1975) 374–377.
[39] G.C. Salzman, M.E. Wilder, J.H. Jett, Light scattering with stream-in-air flow systems, J. Histochem. Cytochem. 27 (1979) 264–267.
[40] H.M. Shapiro, Practical Flow Cytometry, 4th ed., Wiley-Liss, Hoboken, NJ, 2003, pp. 36–38.
[41] T.K. Sharpless, M. Bartholdi, M.R. Melamed, Size and refractive index dependence of simple forward angle scattering measurements in a flow system using sharply-focused illumination, J. Histochem. Cytochem. 25 (1977) 845–856.
[42] S. Smiley, M. Reers, C. Mottolahartshorn, M. Lin, A. Chen, T. Smith, G. Steele, L. Chen, Intracellular heterogeneity in mitochondrial membrane potentials revealed by a J-aggregate-forming lipophilic cation JC-1, Proc. Natl. Acad. Sci. 88 (1991) 3671–3675.
[43] S.P. Srinivas, J.A. Bonanno, E. Larivière, D. Jans, W. Van Driessche, Measurement of rapid changes in cell volume by forward light scattering, Pflugers Arch. 447 (2003) 97–108.
[44] P. Steponkus, Role of the plasma membrane in freezing-injury and cold acclimation, Annu. Rev. Plant Physiol. Plant Mol. Biol. 35 (1984) 543–584.
[45] A. Tárnok, SYTO dyes and histoproteins – myriad of applications, Cytometry A 73 (2008) 477–479.
[46] M.J. Taylor, H.L. Bank, M.J. Benton, Selective killing of leucocytes by freezing: potential for reducing the immunogenicity of pancreatic islets, Diabetes Res. 5 (1987) 99–103.
[47] J. Tchir, J.P. Acker, Mitochondria and membrane cryoinjury in micropatterned cells: effects of cell–cell interactions, Cryobiology 61 (2010) 100–107.
[48] L.W.M.M. Terstappen, B.G. De Groot, G.M.J. Nolten, Physical discrimination between human T-lymphocyte subpopulations by means of light scattering, revealing two populations of T8-positive cells, Cytometry 7 (1986) 178–183.
[49] L.W.M.M. Terstappen, M.R. Loken, Five-dimensional flow cytometry as a new approach for blood and bone marrow differentials, Cytometry 9 (1988) 548–556.
[50] L.W.M.M. Terstappen, V.O. Shah, M.P. Conrad, D. Recktenwald, M.R. Loken, Discriminating between damaged and intact cells in fixed flow cytometric samples, Cytometry 9 (1988) 477–484.
[51] A.J. Ullal, D.S. Pisetsky, C.F. Reich III, Use of SYTO 13, a fluorescent dye binding nucleic acids, for the detection of microparticles in in vitro systems, Cytometry A 77 (2010) 294–301.